Published OnlineFirst March 9, 2010; DOI: 10.1158/1535-7163.MCT-09-0689

Research Article

Molecular Cancer Therapeutics

SB939, a Novel Potent and Orally Active Histone Deacetylase Inhibitor with High Tumor Exposure and Efficacy in Mouse Models of Colorectal Cancer

Veronica Novotny-Diermayr[1], Kanda Sangthongpitag[1], Chang Yong Hu[1], Xiaofeng Wu[1], Nina Sausgruber[1], Pauline Yeo[1], Gediminas Greicius[2], Sven Pettersson[2], Ai Leng Liang[1], Yung Kiang Loh[1], Zahid Bonday[1], Kee Chuan Goh[1], Hannes Hentze[1], Stefan Hart[1], Haishan Wang[1], Kantharaj Ethirajulu[1], and Jeanette Marjorie Wood[1]

Abstract

Although clinical responses in liquid tumors and certain lymphomas have been reported, the clinical efficacy of histone deacetylase inhibitors in solid tumors has been limited. This may be in part due to the poor pharmacokinetic of these drugs, resulting in inadequate tumor concentrations of the drug. SB939 is a new hydroxamic acid based histone deacetylase inhibitor with improved physicochemical, pharmaceutical, and pharmacokinetic properties. *In vitro*, SB939 inhibits class I, II, and IV HDACs, with no effects on other zinc binding enzymes, and shows significant antiproliferative activity against a wide variety of tumor cell lines. It has very favorable pharmacokinetic properties after oral dosing in mice, with >4-fold increased bioavailability and 3.3-fold increased half-life over suberoylanilide hydroxamic acid (SAHA). In contrast to SAHA, SB939 accumulates in tumor tissue and induces a sustained inhibition of histone acetylation in tumor tissue. These excellent pharmacokinetic properties translated into a dose-dependent antitumor efficacy in a xenograft model of human colorectal cancer (HCT-116), with a tumor growth inhibition of 94% versus 48% for SAHA (both at maximum tolerated dose), and was also effective when given in different intermittent schedules. Furthermore, in APC^{min} mice, a genetic mouse model of early-stage colon cancer, SB939 inhibited adenoma formation, hemocult scores, and increased hematocrit values more effectively than 5-fluorouracil. Emerging clinical data from phase I trials in cancer patients indicate that the pharmacokinetic and pharmacologic advantages of SB939 are translated to the clinic. The efficacy of SB939 reported here in two very different models of colorectal cancer warrants further investigation in patients. *Mol Cancer Ther; 9(3); 642–52. ©2010 AACR.*

Introduction

Cancer cells commonly have aberrant patterns of histone modifications. Histone deacetylases (HDAC) are enzymes catalyzing the removal of an acetyl group from a lysine residue. They are classified into four groups: the ubiquitously expressed class I HDACs (HDAC 1, 2, 3 and 8), which are predominantly nuclear localized, and class II HDACs (HDAC 4, 5, 6, 7, 9, and 10) with tissue-specific distribution in both nucleus and cytoplasm. The seven members of the class III HDACs (Sirt 1–7), also called Sirtuins, are structurally not related to other HDACs. HDAC11, the sole member of class IV also shows tissue-specific expression, but is not sharing sufficient homology to be classified as either class I or class II HDAC (for recent reviews, see refs. 1–3).

The acetylation of core histones not only leads to increased accessibility of transcription factors to their target genes but also provides binding domain for bromodomain proteins, which often act as transcriptional coactivators, hence epigenetically influencing transcription (4). Direct acetylation of nonhistone proteins such as transcription factors, nuclear receptors, structural proteins, and chaperone proteins can additionally modify transcription by affecting DNA binding affinity, transcriptional activation, protein stability, and protein-protein interaction (5). The accumulation of acetylated proteins through HDAC inhibition results in a variety of cell type–dependent responses, such as differentiation, induction of cell cycle arrest, apoptosis, as well as altered patterns of gene expression (6)

Changed expression levels of different HDAC enzymes are observed in various types of human cancers (7). Considerable evidence suggests an important role of class I and II HDACs in colorectal cancer. Not only have class I HDACs been shown to play an important role in repressing

Authors' Affiliations: [1]S*Bio Pte. Ltd., Singapore and [2]Department of Cell and Microbiology, Tumor and Cell Biology, Karolinska Institutet, Stockholm, Sweden

Note: Supplementary material for this article is available at Molecular Cancer Therapeutics Online (http://mct.aacrjournals.org/).

V. Novotny-Diermayr and K. Sangthongpitag contributed equally to this work.

Corresponding Author: Veronica Novotny-Diermayr, S*Bio Pte. Ltd., 1 Science Park Road, #05-09 The Capricorn, Singapore Science Park II, Singapore 117528. Phone: 65-6827-5052; Fax: 65-6827-5000. E-mail: veronica_diermayr@sbio.com

doi: 10.1158/1535-7163.MCT-09-0689

Published OnlineFirst March 9, 2010; DOI: 10.1158/1535-7163.MCT-09-0689

intestinal cell maturation, promoting cell proliferation, and survival (8–10) but HDACs from class I and II are also implicated in colon cancer tumorigenesis. Furthermore, both, class I and II HDACs were shown to have increased expression levels, with HDAC2 possibly even acting as a prognostic survival factor for colon cancer patients (7, 11). Taken together, these findings point toward HDACs as particular relevant targets in colon cancer therapy.

There are several different HDAC inhibitors currently in clinical trials, from four different chemical classes, the hydroxamic acids, the cyclic tetrapeptides, benzamides, and the short-chain fatty acids. Most of those that have entered clinical trials have limitations, including low bioavailability, low potency, cardiovascular safety issues, and potential for drug-drug interactions through cytochrome *P*450 inhibition (12, 13). Therefore, there is still a clinical opportunity for efficacious HDAC inhibitors that can provide a better tumor exposure at safe and well-tolerated doses. In this study, we describe SB939 (for structure, see Supplementary Fig. S1, structure activity relationships will be described in a separate article by Wang H. et al.),[3] a highly efficacious HDAC inhibitor with excellent pharmacokinetic properties that is currently in phase I clinical trials (14, 15).

Materials and Methods

Compounds

SB939 and suberoylanilide hydroxamic acid (SAHA) were synthesized in S*BIO. SB939 and SAHA were used as a hydrochloride salt. For *in vitro* studies, compounds were dissolved in DMSO (stock concentration, 10 mmol/L). For *in vivo* studies, dosing solutions used were prepared in 0.5% methylcellulose (w/v) and 0.1% Tween-80 in water for oral dosing. For i.v. injection, SB939 was dissolved in normal saline. SAHA (Vorinostat, Zolinza) was dissolved in *N*,*N*-dimethylacetamide/saline (1:9) at 1 mg/mL. 5-Fluorouracil (5-FU; Sigma Aldrich) was dissolved in saline at a concentration of 4 g/L and sterile filtered.

In vitro Enzyme Assays

All HDAC isoenzymes with the exception of SIRT1 were cloned and expressed in S*BIO. Fluorescence-based HDAC activity assays were done using the HDAC activity assay from Biomol. For all details, see Supplementary Methods.

Cells

Cell lines were obtained from the American Type Culture Collection, with the exception of A2780, ACHN, and MCF7 cells, which were purchased from the European Collection of Cell Culture, and the primary normal human dermal fibroblasts, which were obtained from Cambrex. All cells were cultivated according to the supplier's instructions. Murine peripheral blood mononuclear cells (PBMC) were prepared from whole blood (0.7–1 mL), obtained by cardiac puncture, mixed with 50 μL of a 10% (w/v) EDTA solution, and diluted 1:1 with PBS. This mixture was layered over 2 mL of Histopaque-1083 (Sigma) and centrifuged for 30 min at 400 *g* at room temperature. PBMCs were transferred into a new tube and washed with 800 μL PBS. Cells were spun for 1 min at 5,000 rpm in a microcentrifuge before the lysis of the pellet.

Western Blot Analysis

Cells were washed twice with PBS before lysis in modified radioimmunoprecipitation assay buffer [150 mmol/L NaCl, 50 mmol/L Tris-HCl (pH 7.3), 0.25 mmol/L EDTA (pH 8), 1% sodium deoxycholate, 1% (w/v) Triton X-100, 0.2% (v/v) NaF, 0.1% (w/v) activated Na_3VO_4, 15 μL/mL protease inhibitor cocktail (Sigma), and Garcinol at a final concentration of 10 μmol/L from Biomol]. Snap-frozen tissues were homogenized after adding 0.5 mL of modified radioimmunoprecipitation assay buffer. Cleared lysates were quantified using the protein assay from Bio-Rad according to the manufacturer's protocol. Twenty-five micrograms of protein lysate were separated on 7.5% or 15% SDS-PAGE gels and transferred to polyvinylidene difluoride membranes and processed using standard Western blotting protocols. Antibodies against acetylated (K9/K14) histone H3 (acH3), pRB (S807/S811), $p21^{CIP/Waf}$, cleaved poly ADP ribose polymerase (Asp 214), and anti–rabbit- and anti–mouse-IgG-HRPO were from Cell Signaling Technology, Inc., and β-actin and acetylated tubulin-α were from Sigma. The antibody against retinoblastoma was from Santa Cruz Biotechnology, Inc. and antibodies against total tubulin-α and thymidylate synthase were from Abcam Plc. After developing with enhanced chemiluminescence (GE-Healthcare), the images were captured digitally, using the LAS-3000 Life Science Imager from Fujifilm using exposures between 100 s and 2,000 s at normal sensitivity. Densitometric analysis was done using the MultiGauge software (v3.1) from Fujifilm.

Cell Proliferation Assay

Cells were seeded in 96-well plates at a predetermined optimal density, in the log growth phase, and rested for 24 h (adherent cells) or 2 h (suspension cells), respectively, before treatment with SB939. All experiments were done in triplicates for 96 h, with 1% solvent, using either the CyQUANT Cell proliferation assay kit (Invitrogen Corp.) for adherent cells or the CellTiter96 Aqueous One solution cell proliferation kit (Promega Corp.) for suspension cells, according to the manufacturer's instructions, in a total volume of 100 μL with SB939 concentrations from 100 μmol/L to 1.5 nmol/L in nine serial dilution steps. IC_{50} were determined using the XLfit software (IDBS).

[3] H. Wang, N. Yu, D. Chen, et al. Discovery of (2*E*)-3-{2-Butyl-1-[2-(diethylamino)ethyl]-1*H*-benzimidazol-5-yl}-*N*-hydroxyacrylamide (SB939), an Orally Active Histone Deacetylase Inhibitor with Class-leading Preclinical Profile, in preparation.

Published OnlineFirst March 9, 2010; DOI: 10.1158/1535-7163.MCT-09-0689

Pharmacokinetic Analysis

SB939 was extracted from 50 μL murine plasma or from tissue homogenized in 0.5 mL of PBS. High performance liquid chromatography mass spectrometry analysis was done using a Waters Alliance HT2795/QuattroMicro (Waters Cooperation) with a cooled autosampler and a Luna C18 column (2 × 50 mm), 5 μm (Phenomenex). The mobile phase used was 0.1% formic acid (60%) and high performance liquid chromatography grade methanol (40%) with a flow rate of 0.3 mL/min, a 40°C column temperature, and 40 μL injection volume. The tandem mass spectrometry conditions for multiple reaction monitoring for SB939 were transition of mass to charge ratio (*m/z*) of 359 to *m/z* 100 (SB939) and *m/z* 265 to 232 (SAHA) with a cone voltage of 35 or 25 for SB939 and SAHA, respectively, all in electrospray ionization–positive mode, with a collision energy of 16 eV. The raw data obtained were analyzed in the MassLynx software (Waters Cooperation) and quantified against a standard curve.

Pharmacokinetic parameters were calculated by a noncompartmental method using the WinNonlin 4.0 software (Pharsight Corp.). The area under the plasma concentration versus time curve up to the last quantifiable time point ($AUC_{(0\text{-}t)}$) was obtained by the linear and log-linear trapezoidal summation of the $AUC_{(0\text{-}t)}$ extrapolated to infinity (i.e., $_{AUC(0\text{-}\infty)}$) by adding the quotient of C_{last}/K_{el}, in which C_{last} represents the last measurable time concentration and K_{el} represents the apparent terminal rate constant. K_{el} was calculated by the linear regression of the log-transformed concentrations of the drug in the terminal phase. Absolute bioavailability (F) was calculated as $F = [\text{dose i.v.}] \times AUC_{(0\text{-}\infty)\text{per oral}}/\text{dose per oral} \times AUC_{(0\text{-}\infty)\text{i.v.}}] \times 100$.

HCT-116 Xenograft Mouse Model

Female BALB/c nude mice from the Biological Resource Centre or the Animal Resource Center, 10 to 12 wk of age, were housed in the Biological Resource Centre. Standard protocols were followed, in compliance with the NIH and National Advisory Committee for Animal Research guidelines (Institutional Animal Care and Use Committee approval #0800371). Nude mice were implanted intradermally in the right flank with 5×10^6 HCT-116 cells in 100 μL of serum-free growth medium. Tumor sizes were determined by caliper measurements, and volumes were calculated according to the following formula: Tumor volume (mm^3) = ($w^2 \times l$)/2, in which w is the width and l is the length of the carcinoma in mm.

When the tumor reached a mean volume of ~100 mm^3, the treatment was started by oral gavage (10 mL/kg body weight). The percent tumor growth inhibition (% TGI) was calculated according to the following formula: $\%TGI = (C_{day\ a} - T_{day\ a})/(C_{day\ a} - C_{day\ 1}) \times 100$ [in which $C_{day\ 1}$ is the median tumor volume for control group (vehicle) on day 1, $C_{day\ a}$ is the median tumor volume for control group (vehicle) on day a, and $T_{day\ a}$ is the median tumor volume for treatment group on day a]. Statistical analysis was done with the GraphPad Prism 4 for Windows software (GraphPad Software).

Dosing Schedules

A study with SB939 given once daily for 5 d established that the maximum tolerated dose (MTD) was 100 mg/kg. To determine the dose-response for antitumor efficacy after continuous dosing, mice were treated per oral, once daily for 21 d with 25, 50, 75, or 100 mg/kg of SB939 or vehicle. The antitumor efficacy of SB939 and SAHA was then compared at their MTD (200 mg/kg for SAHA; ref. 16) given once daily for 21 d. To explore intermittent schedules of SB939, mice were dosed for 21 d with either 37.5 mg/kg twice daily, 125 mg/kg every other day, or with 150 mg/kg for 3 d, followed by a 4-d break, for three times (3 d on/4 d off). To test the target efficacy by analysis of acetylated histone H3 (acH3) in tumor and normal tissues, 125 mg/kg every other day was chosen as one of the best intermittent schedules.

Apc^{Min} Intestinal Adenoma Genetic Mouse Model

Male $Apc^{Min/+}$ mice and female C57BL/6 mice (both from The Jackson Laboratory) were housed and bred at the Core Facility for Germfree Research at the Karolinska Institute (Stockholm, Sweden) in compliance with the institutional guidelines (Institutional Animal Care and Use Committee #N102/05 +N110/06) and fed a standard rodent diet. The presence of the heterogeneous *Min* allele in the progeny was confirmed by genotyping, according to instructions provided by The Jackson Laboratory. Mice with the confirmed mutation, between 16 and 20.5 wk of age, with a positive scoring in the hemocult assay (i.e., tested positive at least once in three consecutive assays) were recruited to the experiment. During treatment, mice were injected i.p. with 40 mg/kg of 5-FU in a volume of 200 μL per 20 g body weight, once daily, for 5 d of treatment, followed by a 9-d recovery period and an additional 5 d of treatment. Treatment with SB939 per oral at 50 or 75 mg/kg once daily was given continuously for 21 d. At the last day of the treatment, the small intestine, caecum, and colon were removed; fixed by multiple injections of 4% PBS-buffered formaldehyde into the gut lumen; cut into segments; and spread flat on a plastic film in a formaldehyde bath. Tumor load was measured in a dissection microscope. Assessment and analysis of the samples were done blinded. The Hemocult assay was done using the Hemoplus assay from Sarstedt according to the manufacturer's instructions. The hematocrit was determined by a standard method as described in ref. (17). Statistics were done using the GraphPad Prism 4 for Windows software (GraphPad Software).

Results

Identification of SB939 as a Potent HDAC Inhibitor

SB939 was identified as a potent novel hydroxamate-based inhibitor of HDACs class I, II, and IV, inhibiting the isolated enzymes with a K_i of 19 to 48 nmol/L

Published OnlineFirst March 9, 2010; DOI: 10.1158/1535-7163.MCT-09-0689

(class I), 16 to 247 nmol/L (class II), and 43 nmol/L (class IV), showing an average 2-fold greater potency than SAHA, with the exception of HDAC6. SB939 had no activity against the class III isoenzyme SIRT I (see Table 1). Furthermore, SB939 was shown to have a >100-fold selectivity for HDAC versus Zn-binding non-HDAC enzymes, receptors, and ion channels in a comprehensive screen by MDS pharma services (data not shown).

To test the potency of SB939 on its target in cells, a panel of 29 human cancer cell lines was treated with either SB939 or SAHA, and IC_{50} were determined. The most sensitive cell lines were cutaneous T-cell lymphoma cells and leukemia cells, with IC_{50} values ranging from 50 nmol/L (H9 cutaneous T-cell lymphoma cells) to 170 nmol/L (HEL92.1.7 erythroleukemia cells; see Table 2). Colon and prostate cancer cell lines were among the most sensitive solid tumor cells, with IC_{50} values ranging from 340 to 540 nmol/L. Across all cell lines tested, SB939 was on average 3.5-fold more potent than SAHA. The difference in potency was most prominent for the HCT-116 colon cancer cell line (IC_{50} of 0.48 μmol/L for SB939 compared with SAHA with an IC_{50} of 2.14 μmol/L) and the HL-60 acute myeloid leukemia cell line (SB939: IC_{50}, 70 nmol/L; SAHA: IC_{50}, 530 nmol/L), which is a 6.6- and 7.6-fold higher potency, respectively (Table 2). SB939 did not inhibit the proliferation of normal human dermal fibroblasts at concentrations up to 100 μmol/L (Table 2).

Biomarkers for target efficacy of SB939 were assessed in HCT-116 cells. No signal for acH3 could be detected in vehicle-treated cells (Fig. 1, first two lanes, top), whereas SB939 in concentrations of 0.125 μmol/L and above induced acH3 and the acetylation of α-tubulin after 24 h of treatment. Concentrations of 0.25 μmol/L and above led to decreased retinoblastoma serine phosphorylation on S807/811, an increase of the cyclin-dependant kinase inhibitor $p21^{Cip/WAF}$. The induction of cell cycle arrest was further confirmed by a cell cycle analysis, showing that the number of polyploid cells ($n > 4$) increased dose dependently from 0.25 to 1 μmol/L from an initial 15.8% to 44.6%, respectively, after 24 h treatment with SB939 (shown in Supplementary Fig. S2). The increase in cell cycle arrest goes hand in hand with a dose-dependent increase of cleaved poly ADP ribose polymerase (Fig. 1). In summary, these biomarkers showed target efficacy, induction of cell cycle arrest, and apoptosis.

SB939 Has Superior Pharmacokinetic Properties

To compare the pharmacokinetic properties of SB939 to those of SAHA, nude mice were dosed with 50 mg/kg per oral of either drug, or injected with 10 mg/kg i.v. (data not shown), to calculate bioavailability. Mice were sacrificed at seven different time points between 5 minutes and 24 hours, and HDAC inhibitor concentrations in the plasma were determined. SB939 yielded the highest plasma concentrations (C_{max}) of 2,632 ng/mL and could still be detected 24 hours postdosing. In contrast, SAHA had a much lower C_{max} of 501 ng/mL with the last detectable concentrations measured at 4 hours postdose; the concentration at later time points fell below the detection limits (Fig. 2A and Table 3). The oral bioavailability (F) of SB939 was 34%, which is 4.1-fold higher than for SAHA (F = 8.3%; see Table 3).

SB939 Selectively Accumulates in Tumor Tissue After a Single Oral Dose

To determine the tissue distribution of SB939, nude mice, bearing HCT-116 human colon cancer xenografts, were dosed with 50 mg/kg of SB939 per oral, and the C_{max} was determined in plasma as well as homogenates of liver, lung, kidney, and tumor tissue. Except for tumor, the maximal tissue concentrations were observed at the first time point (10 minutes), indicating rapid distribution from the

Table 1. *In vitro* enzyme activity of SB939 and SAHA

HDAC class	HDAC isoenzyme	SB939 IC_{50} (nmol/L) at the K_m	SB939 K_i* (nmol/L)	SAHA IC_{50} (nmol/L) at the K_m	SAHA K_i* (nmol/L)
I	HDAC1	49	28	110	63
	HDAC2	96	27	157	45
	HDAC3	43	19	75	33
	HDAC8	140	48	326	112
II	HDAC4	56	16	106	30
	HDAC5	47	21	86	39
	HDAC6	1,008	247	165	40
	HDAC7	137	107	154	116
	HDAC9	70	24	108	61
	HDAC10	40	23	81	46
III	SIRT 1	>100,000	>100,000	N.d.†	N.d.
IV	HDAC11	93	43	128	59

*K_i values determined using $IC_{50}/[1 + (\text{concentration of the substrate})/K_m]$.
†Not done.

Published OnlineFirst March 9, 2010; DOI: 10.1158/1535-7163.MCT-09-0689

Table 2. Effects of SB939 and SAHA on cell proliferation of human cancer cell lines

Cell type	Cell line	SB939 IC_{50} (μmol/L)	SD	*n**	SAHA IC_{50} (μmol/L)	SD	*n**
Colon cancer	Colo205	0.54	0.06	8	2.14	0.56	20
	HCT-116	0.48	0.27	5	3.15	1.74	29
Ovarian cancer	A2780	0.48	0.21	4	1.69	0.4	23
Prostate cancer	PC3	0.34	0.06	3	1.28	0.93	27
	DU145	0.53	N.a.	2	0.96	N.a.†	2
Breast cancer	MCF7	0.51	0.1	4	1.04	N.a.	2
	BT549	1.87	0.31	3	4.45	N.a.	2
	MDA-MB231	0.77	0.17	4	2.16	1.45	10
	T47D	0.51	0.14	3	2.38	N.a.	2
Lung cancer (NSCL)	NCI-H460	1.29	0.27	4	3.53	1.6	9
	A549	0.8	0.11	4	1.62	0.39	7
Liver cancer	HEP3B	1.23	N.a.	2	2.13	1.1	6
	PLC/PRF/5	0.9	0.18	3	N.d.‡	N.a.	N.a.
Pancreas cancer	MiaPaCa	0.93	N.a.	2	2.87	0.48	6
Renal cancer	ACHN	0.65	N.a.	2	2.45	N.a.	2
	A498	1.7	N.a.	2	4.25	N.a.	2
	CAKI-1	1.59	N.a.	2	N.d.	N.a.	N.a.
Melanoma	MDA-MB435	0.76	N.a.	2	1.85	1.02	26
Thyroid cancer	ML-1	0.32	N.a.	2	N.d.	N.a.	N.a.
	TT2609	1.07	0.55	4	N.d.	N.a.	N.a.
Leukemia	HL-60	0.07	0.03	3	0.53	0.25	8
	MV4-11	0.1	N.a.	2	0.22	0.16	6
	HEL92.1.7	0.17	N.a.	2	0.31	0.08	5
	MOLT-4	0.12	0.06	3	0.53	N.a.	2
Lymphoma	MJ	0.06	0.02	3	0.47	0.28	3
	H9	0.05	0.02	4	0.16	0.07	4
	HUT78	0.16	0.08	5	0.58	0.23	5
	RPMI8226	0.11	0.001	3	0.31	0.1	3
	L1236	0.29	0.11	4	N.d.	N.a.	N.a.
Primary fibroblasts	NHDF	>100	N.a.	3	N.d.	N.a.	N.a.

Abbreviation: NSCL, non–small cell lung; NHDF, normal human dermal fibroblast.
*Number of independent assays done; each assay was done in triplicates.
†Not applicable.
‡Not done.

systemic circulation (Supplementary Table S1; Fig. 2B). The AUC versus concentration from 0-∞ was calculated to be highest in the tumor tissue (2,953 ng×h/g), followed by kidney, lung, plasma, and liver (for details, see Supplementary Table S2). The half-life ($t_{1/2}$) of SB939 in tumor was also the longest from all tissues (2.31 hours), compared with only 1.43 hours in the plasma (see Supplementary Table S2). In tumor tissue, the maximal concentrations of SB939 were observed 30 minutes postdosing, with concentrations remaining at 136 ng/g tissue, compared with only 11.5 ng/mL in plasma, and between 15.1 and 18.6 ng/g SB939 in other tissues at the 6-hour time point (Fig. 2B, left). This was in contrast to SAHA, which initially showed higher concentration in plasma than in the tumor tissue (581 ng/mL versus 120 mg/g, after dosing with 200 mg/kg SAHA). For SAHA, the C_{max} remained higher in plasma up to 6 hours (81 ng/mL compared with 26 ng/g in tumor tissue) and no accumulation in the tumor tissue could be detected (Fig. 2B, right).

Selection of the Best Dosing Schedule for SB939

The dose range for antitumor efficacy of SB939 was assessed in the HCT-116 murine xenograft model of colon cancer, using nude mice. After 21 days of once daily oral dosing, SB939 showed significant dose-dependent growth inhibition of HCT-116 xenografts for doses from 25 mg/kg up to the MTD of 100 mg/kg. Treatment was well tolerated at all dose levels with no mortalities (Fig. 3A).

To compare the antitumor efficacy of SB939 and SAHA, HCT-116 tumor-bearing mice were dosed with either SB939 or SAHA at their MTD (100 and 200 mg/kg, respectively) given orally once daily for 21 days. In SB939-treated animals, the median tumor volume at the end of the study was 172 mm^3 compared with 550 mm^3

Published OnlineFirst March 9, 2010; DOI: 10.1158/1535-7163.MCT-09-0689

for SAHA and 864 mm^3 for the vehicle control group. This translated to 48% TGI for SAHA at 200 mg/kg ($P < 0.05$) and 94% TGI for SB939 at 100 mg/kg ($P < 0.001$), showing that the better pharmacokinetic properties and high tumor concentrations of SB939 lead to a superior antitumor efficacy (Fig. 3B).

Because HDAC inhibitors that are currently in the clinical trial can only be given intermittently due to a side effect of fatigue, which is considered to be a class effect, the efficacy of SB939 was explored with various intermittent dosing schedules. SB939 was administered to HCT-116-bearing mice in different dosing schedules of either 37.5 mg/kg twice daily, 125 mg/kg every other day, or 150 mg/kg 3 days on and 4 days off for 21 days. The total doses administered over 3 weeks were very similar (between 1,350 and 1,575 mg/kg; see Table 4) and resulted in similar efficacies, with TGIs ranging between 81% and 84%. Tolerability, as indicated by body weight loss, was also very similar with all intermittent schedules. These experiments showed that either a lower continuous dose or a higher intermittent dose can be used with similar efficacies and safety (Fig. 3C and Table 4).

SB939 Selectively Accumulates in Tumor Tissue After Chronic Dosing

The good pharmacokinetic properties and accumulation in tumor tissue were also shown to persist after chronic dosing of SB939 to HCT-116 tumor–bearing mice, using one of the most favorable intermittent dosing schedules (125 mg/kg every other day; Fig. 3C and Table 4). After 21 days of dosing, the highest concentration of SB939 in the tumor far exceeded the plasma concentration at 6 hours (715 ng/g tumor versus 76 ng/mL plasma). At 24 and 48 hours after the last dose, there were still 56 and 24 ng/g SB939 in the tumor, compared with only 4 and 2 ng/mL in the plasma (see Fig. 4A), showing that the tumor tissue remains exposed to SB939 concentrations above the IC_{50} for HCT-116 cells (172 ng/mL or 0.48 μmol/L) for 15 hours and above the *in vitro* IC_{50} for HDAC1 (0.028 μmol/L) for >48 hours after chronic dosing.

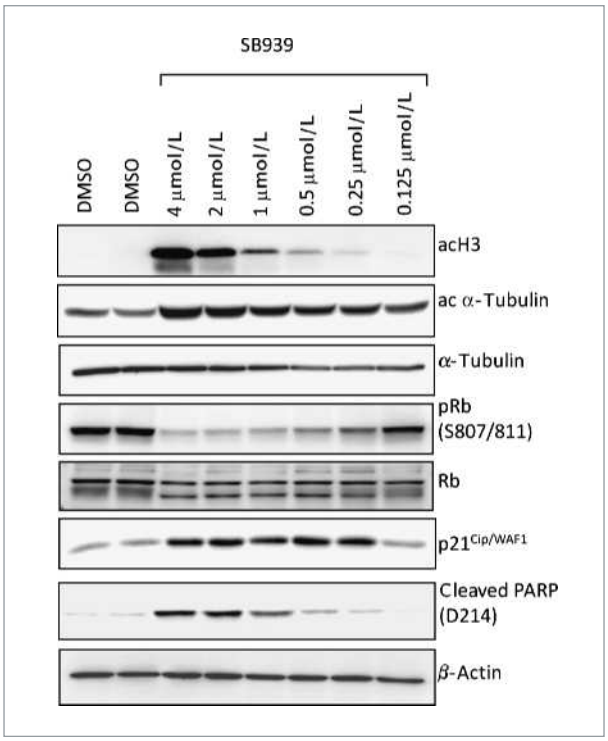

Figure 1. Effects of SB939 on biomarkers in HCT-116 colon cancer cells. HCT-116 colon cancer cells were treated with different concentrations of SB939 for 24 h. Cell lysates were separated on 7.5% or 15% SDS-PAGE gels and Western blots were probed with the antibodies indicated on the right hand side. PARP, poly ADP ribose polymerase.

Target Efficacy in Tumor *In vivo*

To analyze if the favorable pharmacokinetic properties of SB939 over SAHA translated to higher efficacy on the molecular target in different tissues, HCT-116 tumor–bearing mice were dosed orally with single doses of either 50 or 125 mg/kg of SB939 or 200 mg/kg of SAHA. Mice were sacrificed after 1, 3, 8, 16, or 24 hours and target efficacy was determined by measuring acH3 levels in tissues. One hour postdose, acH3 levels in the tumor tissue were similar for 125 mg/kg of SB939 and 200 mg/kg SAHA; however, the effect of SB939 on acH3 was more sustained (up to 16 hours versus up to 8 hours for SAHA; see Fig. 4B and C). The overall pattern of response in murine PBMCs was found to be very similar to the acH3 levels observed in tumor, but the highest acH3 levels were observed 1 hours postdoing in PBMCs compared with 3 hours postdose in tumor lysates.

SB939 Is Efficacious in the Apc^{min} Mouse Model for Colon Carcinoma

Mice carrying mutations in the *Adenomatous polyposis coli* (*Apc*) gene, a gene implicated in the onset and progression of human colon cancer, have been used as genetic models for human colon cancer. The *Min* mutation is a nonsense mutation in the region corresponding to codon 850 of the *Apc* gene, leading to a truncated form of *Apc* (18). Although homozygously lethal, Apc^{min} heterozygotes are born normally, albeit with a reduced life span, and develop a large number of adenomas in the small intestine and fewer in the colon by the age of ~16 weeks, representing the early stages in the development of colorectal cancer. The efficacy of SB939 in this colon cancer model was compared with 5-FU, an antimetabolite used as a standard treatment for human colon cancer. Vehicle mice had an average of 37.5 lesions in the small intestine (Fig. 5A), which were decreased to 22.7 by 5-FU treatment. SB939 at 50 or 75 mg/kg significantly decreased the numbers of lesions by 46% and 53%, respectively, to averages of 20.2 and 17.5 (solid black columns; $P < 0.01$). In the colon, the average tumor numbers were much lower than in the small intestine (1.8 in the vehicle-treated mice), but a 66.7% reduction to 0.6 using 75 mg/kg SB939 was still significant ($P < 0.05$; Fig. 5A, hatched

Published OnlineFirst March 9, 2010; DOI: 10.1158/1535-7163.MCT-09-0689

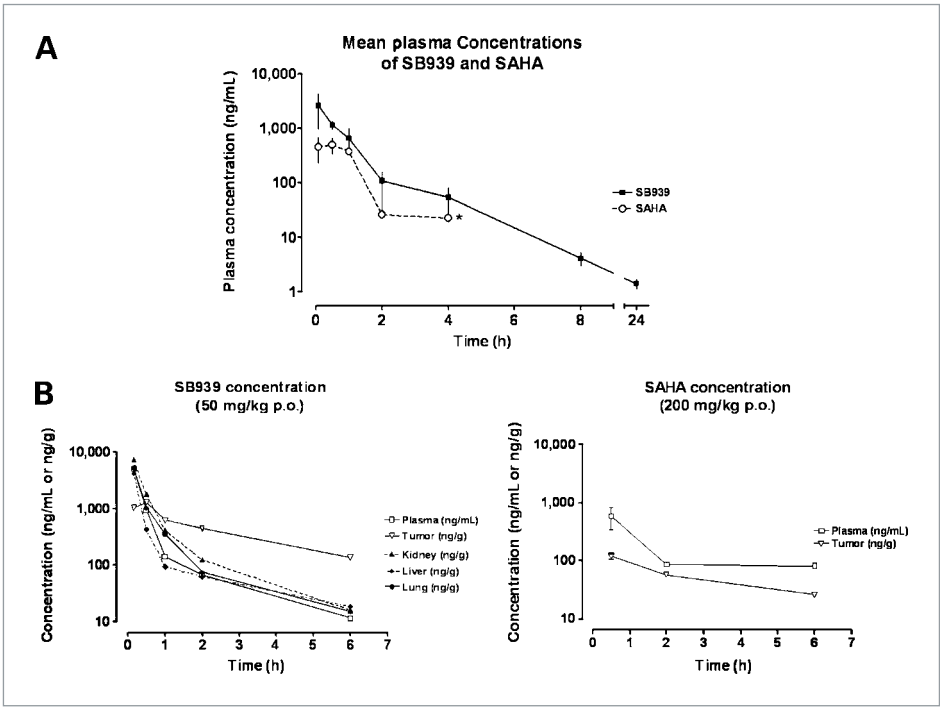

Figure 2. Pharmacokinetic properties of SB939 and SAHA. A, plasma concentration in female BALB/c nude mice, ages 9 to 14 wk, after oral administration of 50 mg/kg of SB939 or SAHA were determined at seven time points (n = 3; points, mean; bars, SD). SAHA values for time points after 4 h are not shown as they were below detection limit. The detection limit is indicated by an asterisk. B, plasma and tissue concentrations of SB939 and SAHA in female BALB/c nude mice, bearing HCT-116 colon cancer xenografts. Mice were treated with 50 mg/kg of SB939 or 200 mg/kg SAHA and the C_{max} was determined from plasma and tissue homogenates at seven time points. Points, mean from two mice, except in which error bars are given (mean values from three mice); bars, SD. $AUC_{0\text{-last}}$, AUC from time zero to the last evaluation time point; $AUC_{0\text{-}\infty}$, AUC extrapolated from time zero to infinity; T_{max}, time to reach C_{max}; F was determined as follows: $AUC_{0\text{-last}}$ per oral (p.o.)/$AUC_{0\text{-last}}$ i.v. × dose i.v./dose per oral × 100.

columns). Cumulative hemocult scores of mice in the different treatment groups during the last 14 days of the study were compared. Vehicle-treated mice scored an average of 1.6 in 78 assays done; the SB939-treated animals scored an average of 0.59 (50 mg/kg) or 0.32 (75 mg/kg) in 76 and 74 assays respectively; and 5-FU treatment gave an average cumulative score of 0.7 in 69 assays done. This confirmed that all treatments led to a highly significant ($P < 0.01$) improvement versus vehicle-treated animals (Fig. 5B). Even at the lower dose of 50 mg/kg SB939, the hemocult scores were lower than for 5-FU. Healthy, C57/BL6 mice have ~40% hematocrit (19), with low hematocrit values being a hallmark of the disease in *Apc*^{min} mice, caused by gastrointestinal bleeding of the lesions. The *Apc*^{min} mice used in our experiments had average hematocrit levels of 25.3%. SB939 (75 mg/kg) increased hematocrit levels to 32%; however, this was not statistically significant from vehicle or 5-FU–treated animals, but treatment with 50 mg/kg SB939 significantly ($P < 0.05$) improved levels to 35.4%, which was not observed after 5-FU (26.2%) treatment (see Fig. 5C).

Table 3. The pharmacokinetic parameters shown in the graph under Fig. 2A were calculated by a noncompartmental method using the WinNonlin 4.0 software. All data shown are averages derived from three individual mice

Parameter	SB939	SAHA
C_{max} (ng/mL)	2,632	501
T_{max} (h)	0.17	0.50
$T_{1/2}$ (h)	2.44	0.75
$AUC_{0\text{-last}}$ (ng×h/L)	1,836	594
$AUC_{0\text{-}\infty}$ (ng×h/L)	1,841	619
F (%)	34	8.3

Discussion

HDAC inhibitors are an emerging class of anticancer drugs with proven efficacy in cutaneous T-cell lymphoma. Promising clinical data have also been described in liquid tumors and some other lymphomas, but efficacy as single agent therapy in solid tumors has been disappointing. Many of the compounds in clinical development have limitations, e.g., low potency, poor pharmaceutical, and pharmacokinetic properties, and undesirable safety profiles limiting the drug exposure that can be achieved in patients (12, 13). Clinical efficacy in solid tumors might be improved with HDAC inhibitors

Published OnlineFirst March 9, 2010; DOI: 10.1158/1535-7163.MCT-09-0689

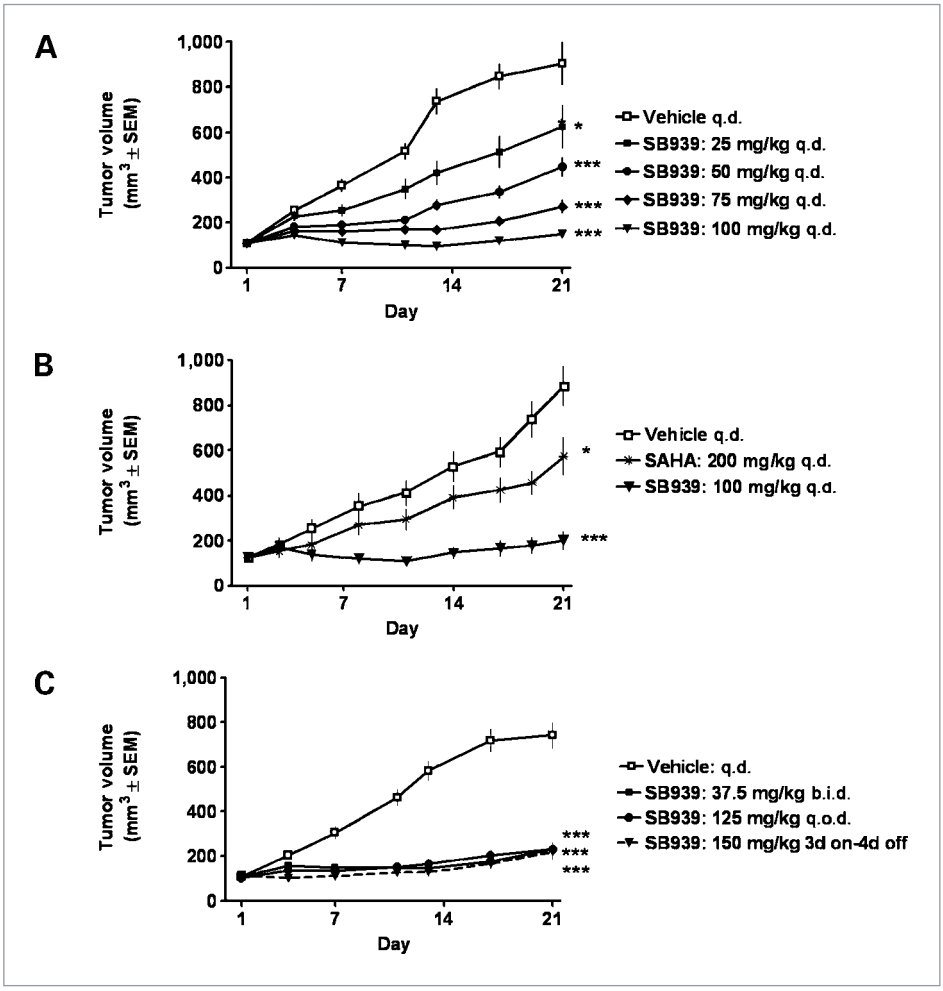

Figure 3. *In vivo* efficacy studies in HCT-116 xenografts to optimize the dosing schedule. A to C, HCT-116 xenografted nude mice were given daily (q.d), twice in day (b.i.d), thrice in week (Monday, Wednesday, Friday; t.i.w.) or 3 d on 4 d off (3d on-4d off) with the indicated doses of SB939, SAHA, or vehicle for 21 d. The doses showing significant TGI in a statistical analysis (ANOVA/ Bonferroni multiple analysis) are indicated with * ($P < 0.05$) or *** ($P < 0.001$). Points, mean tumor volumes; bars, SEM.

that can be dosed high enough to adequately target HDAC enzymes within solid tumor tissue.

SB939, like SAHA, is a pan inhibitor of class I, II, and IV HDACs, but with, on average, a 2-fold higher potency on the HDAC isoenzymes, while not affecting any other zinc-dependent enzymes such as matrix metalloproteinases, hence having a low potential for off-target side effects. In addition, SB939 has a 4-fold increased oral bioavailability and a 3-fold increased half-life compared with SAHA. These excellent pharmacokinetic properties together with the fact that SB939, in contrast to SAHA, accumulates in tumor tissue, translated into a dose-dependent and enhanced antitumor efficacy in a HCT-116 colorectal cancer model. At the MTD, SB939 was

Table 4. The different dosing schedules of the efficacy studies shown under Fig. 2A and B are compared with regard to the total administered dose, TGI, and body weight loss

Dosing Schedule	Dose	Total dose in 3 wk	TGI (day 21)	Max. body weight loss (study day)	Body weight loss (day 21)
Daily	25 mg/kg	525 mg/kg	37%*	9.1% (day 9)	5.7%
Daily	50 mg/kg	1,050 mg/kg	61%***	10.0% (day 17)	7.7%
Daily	75 mg/kg	1,575 mg/kg	76%***	8.6% (day 17)	6.3%
Daily	100 mg/kg	2,100 mg/kg	97%***	16.6% (day 19)	15.5%
Twice a day	37.5 mg/kg	1,575 mg/kg	84%***	14.7% (day 20)	14.4%
Every other day	125 mg/kg	1,375 mg/kg	81%***	6.8% (day 20	6.1%
3d on-4d off	150 mg/kg	1,350 mg/kg	82%***	14.7% (day 13)	9.7%

Published OnlineFirst March 9, 2010; DOI: 10.1158/1535-7163.MCT-09-0689

approximately twice as efficacious as SAHA (the TGI for SAHA at 200 mg/kg was 48% compared with 94% for SB939 at 100 mg/kg) and was also superior to published data with PXD101 (TGI of 51% after 100 mg/kg i.p. once daily for 21 days in a HCT-116 xenograft model; ref. 20).

Although subcutaneous xenografts of human tumors are widely used to show efficacy of cancer drugs, they are established in immunocompromised mice and the tumor microenvironment of the human disease is not truly mimicked. Therefore, SB939 was evaluated in APC^{min} mice, a genetic mouse model of early-stage colon cancer (21). HDAC2, especially, has been shown to play an important role in colon cancer tumorigenesis (22). Both, mice expressing a catalytically inactive HDAC2, when crossed with Apc^{min} mice, or HDAC2 knockout mice when made viable by using a gene trap *LacZ* insertion, develop significantly less adenomas and have shortened crypts and villi (23), all underlining the

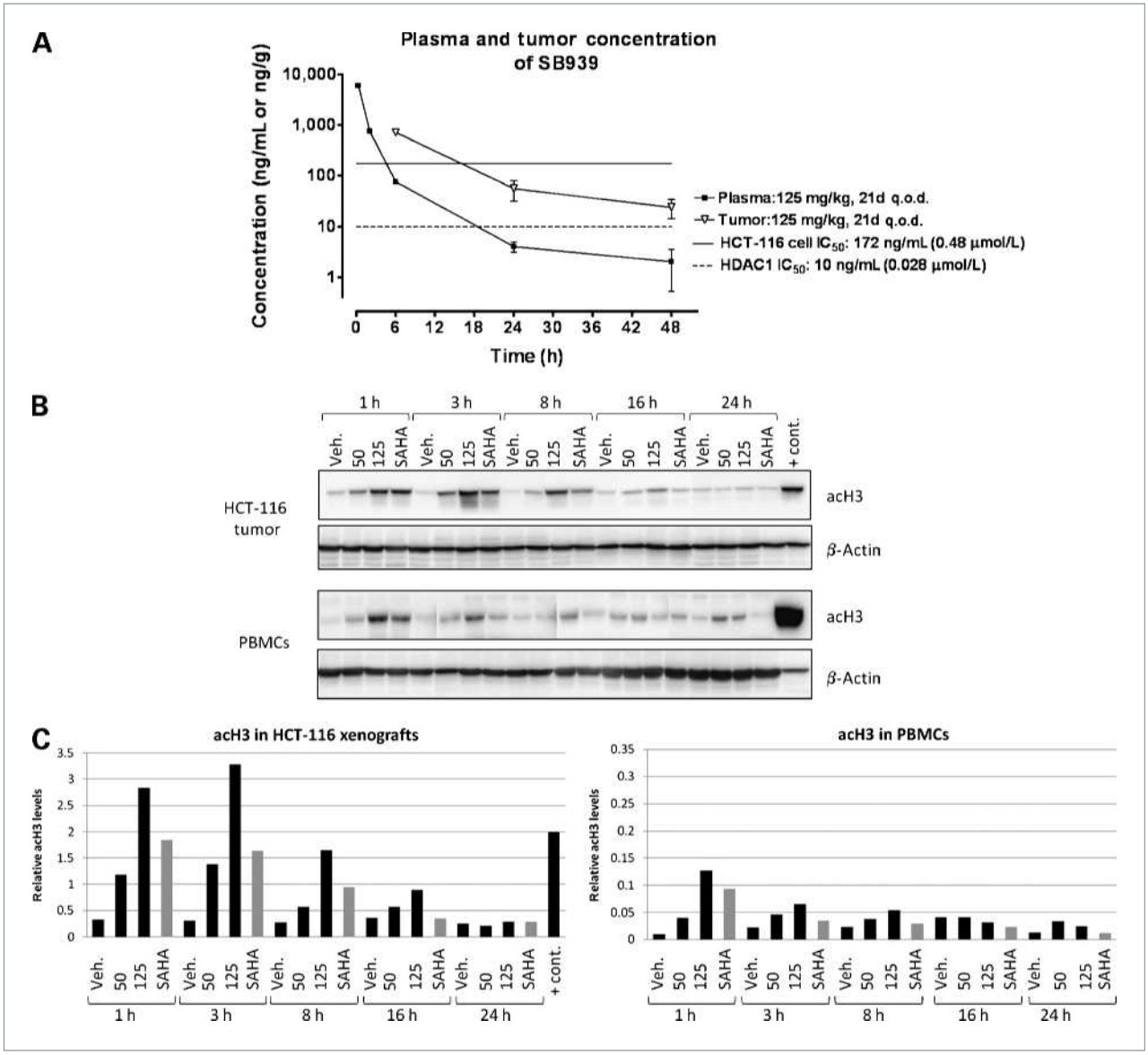

Figure 4. SB939 accumulates in tumor tissue. A, female BALB/c mice engrafted with HCT-116 tumors were treated with 125 mg/kg SB939 thrice in week for 21 d. Thereafter, mice were sacrificed and the concentrations of SB939 in the plasma or the tumor homogenate were analyzed. Data shown for 15 min up to 6 h represent the mean concentration of SB939 of two mice. For 24 and 48 h, the values given are from four mice each; points, mean; bars, SD. B, female BALB/c mice were treated with a single dose of either 50 or 125 mg/kg of SB939 (labeled 50 and 125, respectively) or with 200 mg/kg SAHA and sacrificed at the indicated time points. Five subsequent lanes of the shown Western blot were always run on one Western blot along with two negative controls (vehicles, veh.) in the first two lanes and a positive control (25 µg of HCT-116 cell lysate treated with 2 µmol/L SB939 for 24 h) in the last lane. After digital capture, the positive and negative controls were adjusted to the same level on each blot before assembling the panel. PBMC, peripheral blood mononuclear cell. C, densitometric analysis of the Western blots shown in B. q.o.d., every other day.

Published OnlineFirst March 9, 2010; DOI: 10.1158/1535-7163.MCT-09-0689

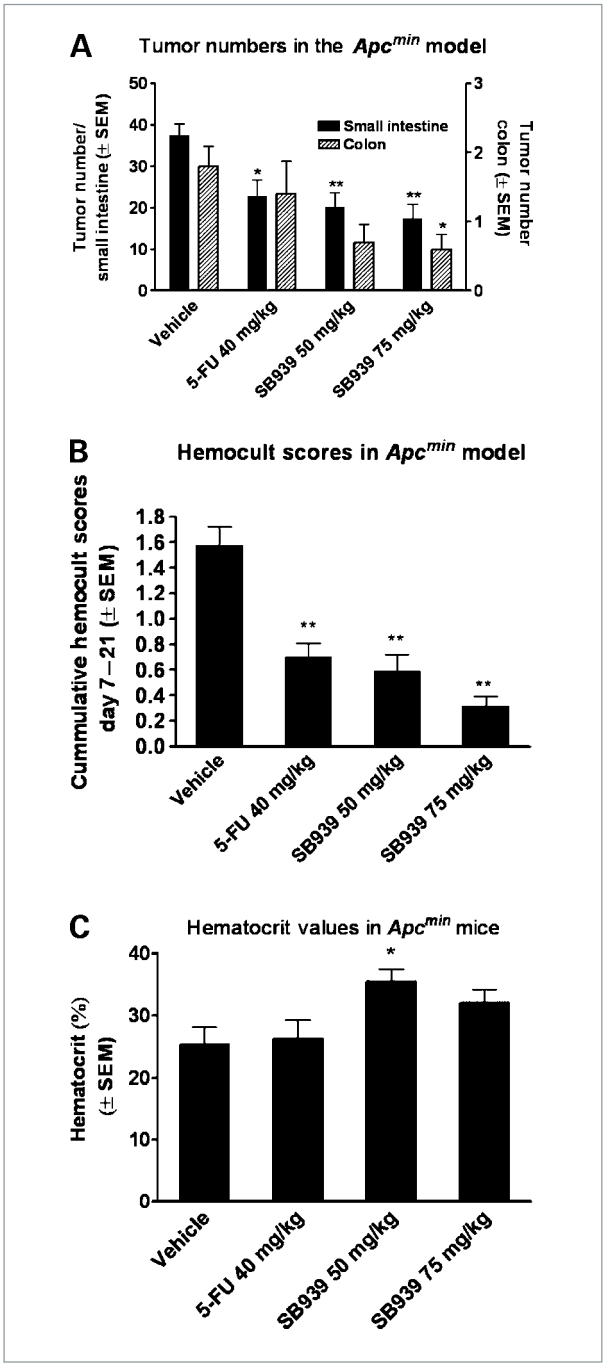

Figure 5. Antitumor activity of SB939 in the Apc^{min} genetic colon cancer mouse model. *Apc^{min}* mice (five male and five female), between 16 and 20.5 wk of age, with established disease, were assigned to four groups and treated with either vehicle, 5-FU, or SB939 for 21 d as described in Material and Methods. A, at the end of the treatment intestine, caecum and colon were removed and fixed, and tumor loads were measured under the dissecting microscope in a blinded fashion. The average number of tumors in the small intestine (solid black columns) and in the colon (cross-hatched columns) is shown. B, the cumulative scores in the hemocult assay from day 7 to the end of the study are given. C, hematocrit values were determined. Asterisks indicate significance (*, $P < 0.05$; **, $P < 0.01$) using the one-way ANOVA Dunett's multiple comparison versus vehicle; columns, mean; bars SEM.

importance of HDACs in the development of colon cancer. Here, we show for the first time that a pan-HDAC inhibitor such as SB939 can dose dependently inhibit adenoma formation in *APC^{min}* mice. Furthermore, the effect with SB939 is greater than the effect with 5-FU, which is one of the standard agents used to treat advanced colorectal cancer. Similar effects on intestinal tumors of *APC^{min}* mice have been achieved using nonsteroid antiinflammatory cyclooxygenase-2 inhibitors (24), suggesting that the efficacy of SB939 in this model may be, in part, due to the antiinflammatory properties that have been described for HDAC inhibitors (25, 26) and which have also been shown for SB939.[4] Proinflammatory cytokines, especially tumor necrosis factor α, which are downregulated by HDAC inhibitor such as SB939, contribute to the inflammatory microenvironment promoting tumor development (27, 28) in *APC^{min}* mice.

Not only was SB939 shown to be efficacious in a genetic model of early-stage colorectal cancer and in a standard xenograft model more representative of later stages of this disease, but was also shown to act synergistically with 5-FU to induce cell death in HCT-116 colon cancer cells *in vitro* (Supplementary Table S1; ref. 29). Such a synergy has recently also been reported for SAHA and LBH589, with the mechanism shown to be the transcriptional repression of thymidylate synthase gene expression (30). In-house, we showed that increasing doses of SB939 also lead to decreasing amounts of thymidylate synthase (Supplementary Fig. S3), as shown in the publication for LBH589 and SAHA (30), indicating that SB939 might act through the same mechanism.

Consistent with the higher sensitivity of leukemias and certain lymphomas toward SB939 in the *in vitro* testing, further profiling of SB939 in *in vivo* models of these tumor types revealed an even higher potency of SB939 compared with the solid tumor models (29), indicating that patients with solid tumors might require higher doses of HDAC inhibitors than patients with leukemias. However, HDAC inhibitors, when dosed continuously, induce fatigue, a side effect that is thought to be mechanism related and necessitates intermittent dosing schedules (31). SB939 was shown to be effective and well tolerated in a colon cancer model when given in various intermittent dosing schedules. This may be due to the ability of this compound to accumulate in tumor tissue, therefore providing adequate exposure of the tumor tissue. Hence, SB939 has the potential to be more effective in solid tumor patients than other HDAC inhibitors with poor pharmacokinetic properties and side effects that limit dose.

In summary, we report the preclinical profile of SB939, a potent HDAC inhibitor with superior pharmacokinetic properties, leading to a selective enrichment of the drug in the tumor, with high efficacy and favorable tolerability in two different mouse models of colorectal cancer. The

[4] Unpublished data.

Published OnlineFirst March 9, 2010; DOI: 10.1158/1535-7163.MCT-09-0689

data from the studies described in this article provided the basis for the selection of the dosing schedules for the ongoing phase I trials with SB939. Preliminary results from the phase I trials indicate that the superior preclinical pharmacokinetic, pharmacodynamic, and safety properties of SB939 are translated to the clinic (32, 33). Our data also provide an attractive rationale for clinical trials with SB939 in colorectal cancer.

Disclosure of Potential Conflicts of Interest

V. Novotny-Diermayr, K. Sangthongpitag, C.Y. Hu, X. Wu, N. Sausgruber, P. Yeo, A.L. Liang, Y.K. Loh, Z. Bonday, K.C. Goh, H. Hentze, S. Hart, H. Wang, K. Ethirajulu, and J.M. Wood are employees of S*Bio Pte. Ltd.

Acknowledgments

We thank Chitra Amalini, Evelyn Goh, Miah Kiat Goh, Siok Kun Goh, Vasantha Nayagam, Tony Ng, Lee Sun New, Muhammed Khalid Prasha, Reddy Venkatesh, Xukun Wang, Liu Xin, and Peizi Zeng for their excellent technical help and Walter Stuenkel for initiating this project.

The costs of publication of this article were defrayed in part by the payment of page charges. This article must therefore be hereby marked *advertisement* in accordance with 18 U.S.C. Section 1734 solely to indicate this fact.

Received 07/28/2009; revised 11/24/2009; accepted 01/04/2010; published OnlineFirst 03/02/2010.

References

1. Pan LN, Lu J, Huang B. HDAC inhibitors: a potential new category of anti-tumor agents. Cell Mol Immunol 2007;4:337–43.
2. Minucci S, Pelicci PG. Histone deacetylase inhibitors and the promise of epigenetic (and more) treatments for cancer. Nat Rev Cancer 2006;6:38–51.
3. Witt O, Deubzer HE, Milde T, Oehme I. HDAC family: What are the cancer relevant targets? Cancer Lett 2009;8:8–21.
4. Haberland M, Montgomery RL, Olson EN. The many roles of histone deacetylases in development and physiology: implications for disease and therapy. Nat Rev Genet 2009;10:32–42.
5. Glozak MA, Sengupta N, Zhang X, Seto E. Acetylation and deacetylation of non-histone proteins. Gene 2005;363:15–23.
6. Marks PA, Richon VM, Rifkind RA. Histone deacetylase inhibitors: inducers of differentiation or apoptosis of transformed cells. J Natl Cancer Inst 2000;92:1210–6.
7. Ellis L, Atadja PW, Johnstone RW. Epigenetics in cancer: targeting chromatin modifications. Mol Cancer Ther 2009;8:1409–20.
8. Wilson AJ, Byun DS, Popova N, et al. Histone deacetylase 3 (HDAC3) and other class I HDACs regulate colon cell maturation and p21 expression and are deregulated in human colon cancer. J Biol Chem 2006;281:13548–58.
9. Tou L, Liu Q, Shivdasani RA. Regulation of mammalian epithelial differentiation and intestine development by class I histone deacetylases. Mol Cell Biol 2004;24:3132–9.
10. Zhu P, Martin E, Mengwasser J, Schlag P, Janssen KP, Gottlicher M. Induction of HDAC2 expression upon loss of APC in colorectal tumorigenesis. Cancer Cell 2004;5:455–63.
11. Weichert W, Roske A, Niesporek S, et al. Class I histone deacetylase expression has independent prognostic impact in human colorectal cancer: Specific role of class I histone deacetylases *in vitro* and *in vivo*. Clin Cancer Res 2008;14:1669–77.
12. Glaser KB. HDAC inhibitors: clinical update and mechanism-based potential. Biochem Pharmacol 2007;74:659–71.
13. Elaut G, Rogiers V, Vanhaecke T. The pharmaceutical potential of histone deacetylase inhibitors. Curr Pharm Des 2007;13:2584–620.
14. Lee MJ, Kim YS, Kummar S, Giaccone G, Trepel JB. Histone deacetylase inhibitors in cancer therapy. Curr Opin Oncol 2008;20:639–49.
15. Beckers T, Burkhardt C, Wieland H, et al. Distinct pharmacological properties of second generation HDAC inhibitors with the benzamide or hydroxamate head group. Int J Cancer 2007;121:1138–48.
16. Cohen LA, Amin S, Marks PA, Rifkind RA, Desai D, Richon VM. Chemoprevention of carcinogen-induced mammary tumorigenesis by the hybrid polar cytodifferentiation agent, suberanilohydroxamic acid (SAHA). Anticancer Res 1999;19:4999–5005.
17. Strumia MM, Sample AB, Hart ED. An improved micro hematocrit method. Am J Clin Pathol 1954;24:1016–24.
18. Heyer J, Yang K, Lipkin M, Edelmann W, Kucherlapati R. Mouse models for colorectal cancer. Oncogene 1999;18:5325–33.
19. Perkins S, Verschoyle RD, Hill K, et al. Chemopreventive efficacy and pharmacokinetics of curcumin in the min/+ mouse, a model of familial adenomatous polyposis. Cancer Epidemiol Biomarkers Prev 2002;11:535–40.
20. Tumber A, Collins LS, Petersen KD, et al. The histone deacetylase inhibitor PXD101 synergises with 5-fluorouracil to inhibit colon cancer cell growth *in vitro* and *in vivo*. Cancer Chemother Pharmacol 2007;60:275–83.
21. Yamada Y, Mori H. Multistep carcinogenesis of the colon in Apc(Min/+) mouse. Cancer Sci 2007;98:6–10.
22. Morin PJ, Vogelstein B, Kinzler KW. Apoptosis and APC in colorectal tumorigenesis. Proc Natl Acad Sci U S A 1996;93:7950–4.
23. Zimmermann S, Kiefer F, Prudenziati M, et al. Reduced body size and decreased intestinal tumor rates in HDAC2-mutant mice. Cancer Res 2007;67:9047–54.
24. Swamy MV, Patlolla JM, Steele VE, Kopelovich L, Reddy BS, Rao CV. Chemoprevention of familial adenomatous polyposis by low doses of atorvastatin and celecoxib given individually and in combination to APCMin mice. Cancer Res 2006;66:7370–7.
25. Leoni F, Fossati G, Lewis EC, et al. The histone deacetylase inhibitor ITF2357 reduces production of pro-inflammatory cytokines *in vitro* and systemic inflammation *in vivo*. Mol Med 2005;11:1–15.
26. Leoni F, Zaliani A, Bertolini G, et al. The antitumor histone deacetylase inhibitor suberoylanilide hydroxamic acid exhibits antiinflammatory properties via suppression of cytokines. Proc Natl Acad Sci U S A 2002;99:2995–3000.
27. Mantovani A, Allavena P, Sica A, Balkwill F. Cancer-related inflammation. Nature 2008;454:436–44.
28. Mantovani A, Pierotti MA. Cancer and inflammation: a complex relationship. Cancer Lett 2008;267:180–1.
29. Sangthongpitag K, Wu X, Khng H, et al. 162 POSTER Pharmacological profile of SB939, a novel, potent and orally active histone deacetylase inhibitor. Eur J Cancer Suppl 2006;4:abstract 52.
30. Fazzone W, Wilson PM, Labonte MJ, Lenz HJ, Ladner RD. Histone deacetylase inhibitors suppress thymidylate synthase gene expression and synergize with the fluoropyrimidines in colon cancer cells. Int J Cancer 2009;125:463–73.
31. Prince HM, Bishton MJ, Harrison SJ. Clinical studies of histone deacetylase inhibitors. Clin Cancer Res 2009;15:3958–69.
32. Yong WP, Goh BC, Ethirajulu K, et al. A phase I dose escalation study of oral SB939 when administered thrice weekly (every other day) for 3 weeks in a 4-week cycle in patients with advanced solid malignancies. Eur J Cancer 2008;6:abstract 413.
33. Yong W, Goh B, Toh H, et al. Phase I study of SB939 three times weekly for 3 weeks every 4 weeks in patients with advanced solid malignancies. J Clin Oncol 2009;27:abstract 2560.

AACR American Association for Cancer Research

Molecular Cancer Therapeutics

SB939, a Novel Potent and Orally Active Histone Deacetylase Inhibitor with High Tumor Exposure and Efficacy in Mouse Models of Colorectal Cancer

Veronica Novotny-Diermayr, Kanda Sangthongpitag, Chang Yong Hu, et al.

Mol Cancer Ther 2010;9:642-652. Published OnlineFirst March 9, 2010.